ELSEVIER

Journal of Alloys and Compounds 323–324 (2001) 376–379

Journal of ALLOYS AND COMPOUNDS

www.elsevier.com/locate/jallcom

A new crystalline host for lasing Ln^{3+} ions: disordered calcium–lutetium fluoride

A.A. Kaminskii[a,*], D. Jaque[b], J.J. Romero[c], J. García Solé[c], A.V. Butashin[a]

[a]*Institute of Crystallography, Russian Academy of Sciences, Leninsky pr. 59, Moscow, 117333, Russia*

[b]*Departamento de Física de los Materiales, Facultad de Ciencias Físicas, Universidad Complutense de Madrid, Ciudad Univesitaria, 28040 Madrid, Spain*

[c]*Departamento de Física de Materiales, C-IV, Universidad Autónoma de Madrid, Cantoblanco, 28049 Madrid, Spain*

Abstract

A new crystalline host for laser Ln^{3+} ions is developed based on the $CaLu_2F_8$ crystal. Laser oscillation at 1.05 μm is demonstrated for the Nd^{3+} doped crystal, corresponding to the $^4F_{3/2} \rightarrow {}^4I_{11/2}$ laser channel. Spectroscopic laser gain experiments have been used to estimate the emission cross section as well as the internal loss factor associated to crystal lattice. The broad bands together with the relative high loss factor are explained in terms of the partial disorder existing in crystal structure.

Keywords: Insulators; Optical materials; Luminescence

1. Introduction

Since the discovery of Ln^{3+} doped disordered fluoride laser crystals, they have been considered as very attractive media for laser drivers in the laser fusion reactors [1]. Disordered fluorides crystallize in the MF_2–RF_3 system (M=Ca, Sr, Ba and R=Ln) with structures derived from cubic fluorite (CaF_2) in the MF_2-rich parts and from trigonal tysonite (LaF_3, space group D^4_{3h}, $Z=6$) in the RF_3-rich parts [2].

Insulating host crystals containing Lutetium are attractive for activation with La^{3+} ions because of several reasons: absence of UV, visible and infrared absorption lines; similar crystal chemistry to other lanthanide crystals, important to incorporate Ln^{3+} ions. Finally, these host crystals usually have higher mechanical and optical strength and stronger resistance to thermal hydrolysis than other rare earth doped laser crystals [3].

In addition, these crystals present a partial disordered structure [2,4]. This partial disorder results in broadening of the optical bands. Broad absorption bands avoid a precise control of pump wavelength, which simplifies the pump source design. On the other hand, broad emission bands can be used to generate tunable laser sources [3]

In this paper we report on the basic spectroscopic properties (luminescence lifetime, branching ratios) of Nd^{3+} ions in calcium–lutetium fluoride, extending our previous work on the same material [5]. Continuous wave laser gain experiments ($^4F_{3/2} \rightarrow {}^4I_{11/2}$ laser channel) under Ti:sapphire pumping are used to estimate the internal loss factor.

2. Experimental

Fig. 1 shows the phase diagram of the CaF_2–LuF_3 system. In this diagram the A zone corresponds to a solid solution with fluorite structure, whereas the B zone corresponds to the disordered compound $CaLu_2F_8$ derived from the tysonite [4,5].

Crystals doped with Nd^{3+} ions (<1 at.%) were grown by the Bridgman–Stockbarger method from a Lutetium-rich part of the CaF_2–LuF_3 system. By inspection of Fig. 1, this corresponds to a LuF_3 concentration of about 67 mol.%. Graphite furnace and crucibles in a fluorinating atmosphere were used. The growing speed was 2 mm/h resulting in single crystals of several cm^3. Although at present precise structural data are not available for the $CaLu_2F_8$ crystal, we can postulate partial disordering of its crystal structure because of a random occupancy, by the Ca^{2+} and Lu^{3+} cations, of the relevant La^{3+} sites in the tysonite structure, and also because of a random occupancy

*Corresponding author. Fax: +7-95-135-1011.

0925-8388/01/$ – see front matter
PII: S0925-8388(01)01057-X

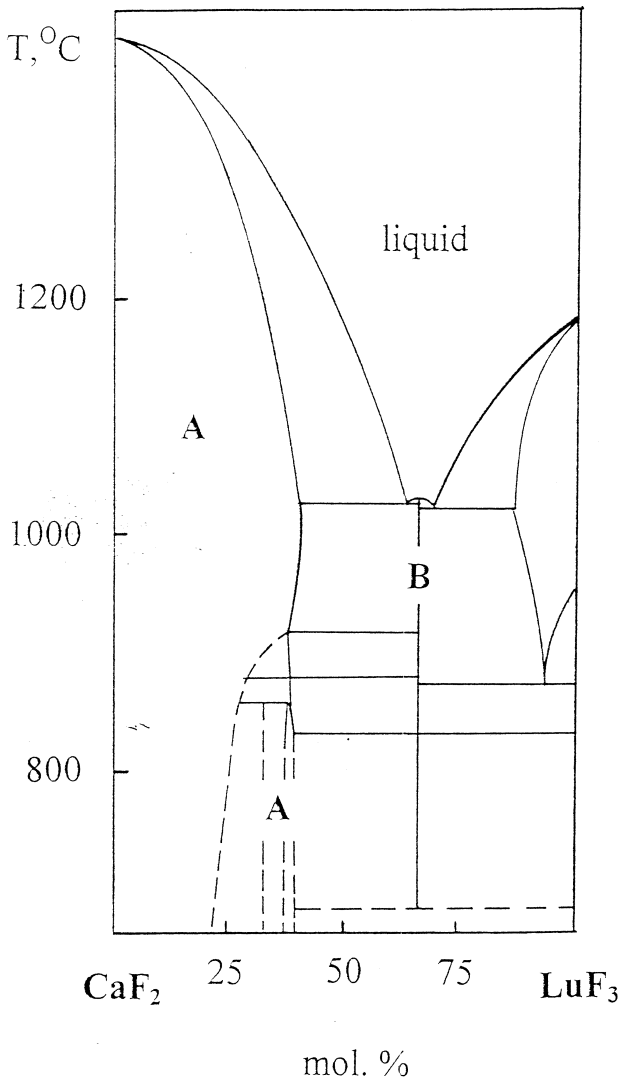

Fig. 1. Phase diagram of the CaF_2–LuF_3 system. A-zone corresponds to a solid solution with the fluorite structure. B-zone corresponds to the disorder compound $CaLu_2F_8$ derived from the tysonite.

by the F centers and vacancies of the relevant anion sites [4,6]. Consequently, introduction of Nd^{3+} ions in this crystal gives place to Nd-centers with different structures, leading to inhomogeneously broadened absorption and emission bands. The same features were reported for the Nd^{3+} doped CaF_2–LuF_3 solid solutions (LuF_3 concentrations around 10 mol.%) [4].

Crystals were cut and polished up to laser quality. Final crystal length was 1.8 mm. The optical absorption spectra were measured with an Hitachi spectrophotometer (model U-3501). For the fluorescence (excitation and emission) spectra and laser gain experiments a Ti:Sapphire (Spectra Physics, model 3900) tunable laser was used. Experiments under pulsed excitation were performed by using a high power (20 mJ, 10 ns pulse width) optical parametric oscillator (MOPO, Spectra Physics model 730). The luminescence was dispersed by a 500 M SPEX monochromator (spectral resolution = 0.05 nm) and detected with a cooled photomultiplier or a calibrated Ge detector (depending upon the spectral range). The signals were recorded by using an EG & G lock-in amplifier. Decay time measurements were performed using the averaging facilities of a Tektronix 2400 digital storage oscilloscope. For these experiments, monochromator slits were opened so that the spectral resolution was around 2 nm. For laser gain experiments, a hemispherical end-pumped cavity, composed of a plane input mirror (high reflectance at 1 μm) and a 10-cm radius of curvature output mirror (99% reflectance at 1 μm), was used. The pump beam from the Ti:Sapphire laser was focused into the sample by a 5-cm focal lens. Spectral shape of the infrared laser beam was analyzed in real time by means of an Optical Multichannel Analyzer (Otsuka MCPD 1100).

3. Results and discussion

3.1. Basic spectroscopy

Fig. 2a shows the emission spectrum in the 800–1500 nm spectral range (excitation was set to 807 nm, where

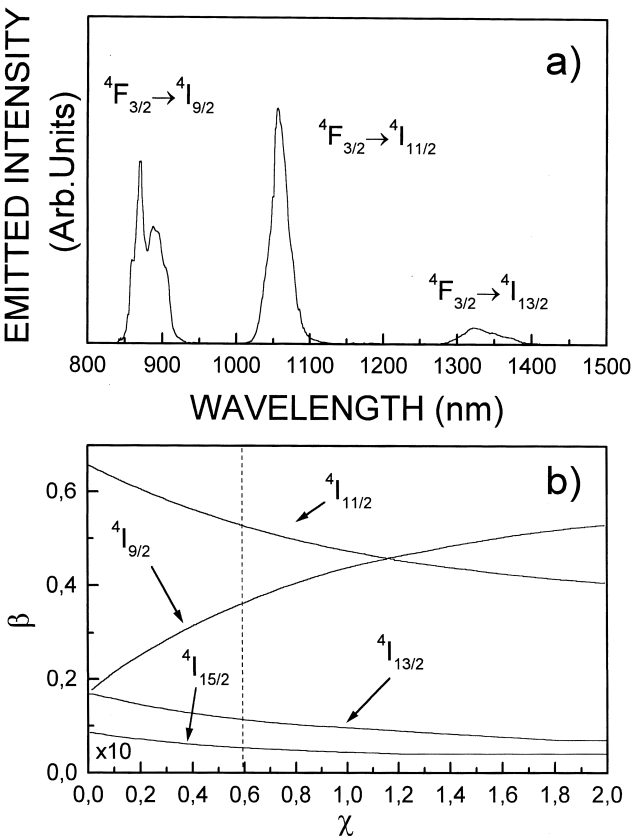

Fig. 2. (a) Emission spectra obtained at room temperature after 807 nm excitation. (b) Dependence of the radiative branching ratios of the $^4F_{3/2}$ state as a function of the spectroscopic quality parameter as defined in text.

absorption spectrum peaks). Only radiative emissions departing from metastable $^4F_{3/2}$ state are detected. The final state corresponding to each band is indicated in the figure. The $^4F_{3/2} \rightarrow {}^4I_{15/2}$ transition is not shown due to its low emission intensity, as well as to experimental limitations. The emission bands are very broad, which is an indication of the crystal disorder, producing a large number of different environments for the Nd^{3+} ions. From this figure the branching ratios can be experimentally obtained by integrating the corresponding emission and then dividing by the total integrated area. For this purpose a calibrated Ge detector was used to correct by the spectral response. The β-values obtained are 0.35, 0.53 and 0.11 for the transitions from the $^4F_{3/2}$ state to the $^4I_{9/2}$, $^4I_{11/2}$ and $^4I_{13/2}$ states, respectively.

According to Ref. [3] the probability of spontaneous transitions $A_{JJ'}$ for the various $^4F_{3/2} \rightarrow {}^4I_{J'}$ channels mainly depends on the intensity parameters Ω_t, $t=4$, 6. This is because the matrix element $\langle\|U^{(2)}\|\rangle$ for transitions between these states is zero. Hence the branching ratios $\beta_{JJ'}$ are dependent of only one parameter, the spectroscopic-quality parameter (χ), defined as [3]:

$$\chi\left(^4F_{3/2}\right) = \frac{\Omega_4}{\Omega_6} \tag{1}$$

Fig. 2b shows the analytical dependence of the branching ratios as a function of χ. Once the branching ratios have been experimentally determined, the spectroscopic quality parameter can be estimated. By inspection of Fig. 2b and using the value of β experimentally obtained (dotted line in Fig. 2b), we found $\chi \approx 0.6$.

The $^4F_{3/2}$ fluorescence lifetime, τ_F, has been measured at room temperature. Fig. 4 shows the temporal behavior corresponding to the luminescence departing form the metastable state $^4F_{3/2}$. The temporal decay can be nicely fitted to a single exponential decay (solid line in Fig. 3). This fact roughly indicates that in spite of the different Nd^{3+} centers (due to the partial disorder) the total de-excitation probability is not affected within the experimental accuracy [7]. In addition, the obtained lifetime ($\sim 430 \pm 30$ μs) was independent on both the excitation and emission wavelengths.

The emission cross section, σ_{em}, for the $^4F_{3/2} \rightarrow {}^4I_{11/2}$ laser channel is [3]:

$$\sigma_{em} = \frac{\lambda_l^2 \cdot \beta}{8 \cdot \pi \cdot n^2 \cdot \Delta\nu_l \cdot \tau_F} \tag{2}$$

where β is the $^4F_{3/2} \rightarrow {}^4I_{11/2}$ branching ratio, $\Delta\nu_l = c \cdot \Delta\tilde{\nu}_l$ is the effective width of the inhomogeneously broadened $^4F_{3/2} \rightarrow {}^4I_{11/2}$ luminescence band ($\Delta\tilde{\nu}_l \approx 190$ cm^{-1}), τ_F is the fluorescence lifetime, $n=1.50$ is the refractive index and λ_l the laser wavelength (maximum at the emission spectrum in Fig. 2a). The obtained emission cross section was 4.2×10^{-20} cm^2, in the same order but lower than the emission cross section determined for other Nd^{3+} doped laser crystals [3].

3.2. Laser gain experiments

Fig. 4 shows the infrared laser power as a function of the absorbed pump power. Laser oscillation was achieved for a spread range of pump wavelengths, because of the broad absorption band around 800 nm (not shown here for the sake of brevity). This is a very positive characteristic, since stabilization of the pump wavelength is not necessary, simplifying the pump system.

From Fig. 4, the absorbed pump power at threshold was ~200 mW, which is higher than those obtained for other Nd^{3+} doped laser crystals under the same experimental conditions [8]. This relatively high pump power at threshold can be explained in terms of the poor optical quality of our laser element (high internal loss factor). The internal loss factor, L, can be estimated from laser gain experi-

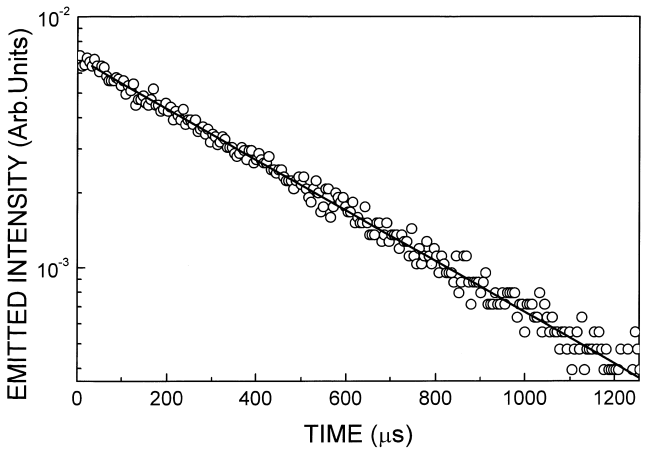

Fig. 3. Time evolution of the $^4F_{3/2}$ luminescence after pulsed pumping at 890 nm. Dot are experimental data and line is a single exponential fit.

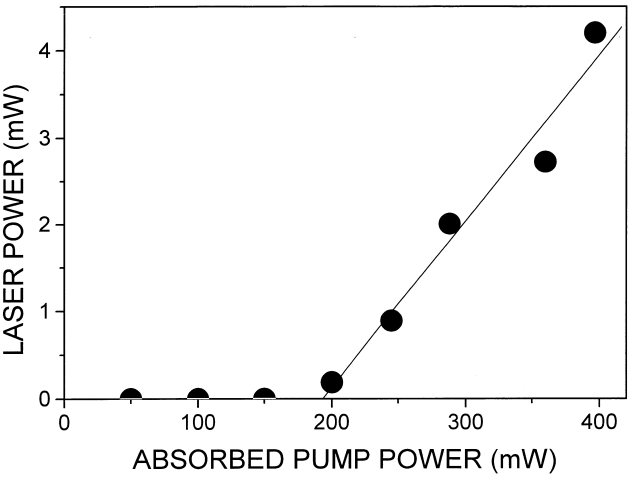

Fig. 4. Dependence of infrared laser power on the absorbed pump power. Doted line is a linear fit.

ments if the laser slope efficiency (η) for a given output mirror transmittance (T) is known. In our experimental conditions (Gaussian beams) the laser slope efficiency can be written as [9]:

$$\eta = 0.75 \cdot \frac{T}{T+L} \quad (3)$$

From Fig. 4 the laser slope efficiency obtained is ~2%. By substitution in Eq. (3) and taking into account the absence of anti-reflection coatings on crystal faces we have found that the internal loss factor is as high as 30% cm^{-1} ($L = 10.8\%$). This value is about ten times higher than those usually obtained for other Nd^{3+} doped crystals [8]. As it was mentioned before this is attributed to the crystal disordered structure. Nevertheless optically homogeneous crystals could be obtained by a more precise determination of their congruent composition and by optimizing the cooling procedure after the end of crystallization.

4. Conclusions

We have performed basic spectroscopic and laser gain experiments on a new Nd^{3+} doped $CaLu_2F_8$ laser crystal. The main physical parameters of relevance for laser oscillation (emission cross section, internal loss factor, spectroscopic quality parameter and fluorescence lifetime) corresponding to the $^4F_{3/2} \rightarrow {}^4I_{11/2}$ laser channel have been estimated. Crystal partial disorder structure produces broad emission and absorption bands as well as high internal losses.

Acknowledgements

This work has been sponsored by the Comisión Interministerial de Ciencia y Tecnología (CICyT) under project No. PB97-0033. All the authors wish to state that their research work was significantly incentivated by the cooperation within the 'Laser Crystals and Precise Laser Systems' Joint Open Laboratory.

References

[1] A.A. Kaminskii (Ed.), Laser Crystals, Nauka, Moscow, 1975.
[2] B.P. Sobolev, P.P. Fedorov, J. Less-Common Met. 60 (1978) 33.
[3] A.A. Kaminskii, Crystalline Lasers, CRS Press, New York, 1996.
[4] D.J.M. Bevan, O. Greis, Rev. Chim. Min. 15 (1978) 346.
[5] A.A. Kaminskii, A.V. Butashin, L.E. Li, D. Jaque, J. García Solé, Quantum Electronics 29 (1999) 375.
[6] A.A. Kaminskii, B.P. Sobolev, Z.I. Zhmurova, S.E. Sarkisov, Neorgan. Mater. 20 (1984) 869.
[7] B. Henderson, G.F. Imbusch, Optical Spectroscopy of Inorganic Solids, Oxford Science Publications, Claderon Press, Oxford, 1989.
[8] D. Jaque, J. Capmany, J.A. Sanz García, A. Brenier, G. Boulon, J. García Solé, Optical Mat. 13 (1999) 147.
[9] W.P. Risk, R. Pon, W. Lenth, Appl. Phys. Lett. 54 (1989) 1625.